

Modifications of the HEX Program for Fast Automatic Resolution of PIXE-Spectra

Gerd I. Johansson

Department of Nuclear Physics, Lund Institute of Technology, Sölvegatan 14, S-223 62 Lund, Sweden

The computer program 'HEX' for resolving PIXE-spectra has been modified. By irradiating standard foils, the escape peak ratios for x-ray peaks in the energy interval 3.3–10.6 keV have been measured. The results have been compared with theoretical calculations and experimental results of other research groups. The escape peaks have been included in the computer code. Pile-up peaks in the x-ray spectrum are also fitted by the modified computer program. This procedure is independent of the count rate and the pile-up interval. In addition, an effective routine for rejecting small x-ray peaks has been developed.

INTRODUCTION

A fast reliable computer program is essential for the full use of PIXE-analysis. One approach, the computer program HEX (earlier called REX), was explored by H.C. Kaufmann *et al.*^{1–3} The development of HEX permitted good progress to be made in routine fast resolution of PIXE-spectra especially these from thin samples of ambient aerosols. The use of PIXE-analysis has, however, expanded, thus increasing and changing the requirements on the computer program for spectrum resolution. The analysis of different kinds of samples containing many elements places great demands upon the ability to resolve peaks. To avoid erroneous results, it is essential that means of handling the escape peaks are included in the computer code. To limit computer analysis time, it is necessary to develop routines for rejecting undesirable peaks and elements, when analysing unknown samples.

One of the advantages of PIXE is its short analysis time. Its speed can be further increased by increasing the count rate, at the expense of larger pile-up peaks which must in turn be handled by the computer program.

A version of HEX (HEX78) has been modified in response to the requirements described resulting in a new version HEXLUND81.

THE COMPUTER PROGRAM HEX

The computer program HEX is based on a physical model describing an x-ray spectrum as Gaussian distribution peaks on a continuum. The model uses experimental information from the literature, e.g. the relative intensities and energies of x-ray peaks, so as to increase the speed of spectrum resolution. By using a least squares algorithm similar to that suggested by Marquardt,⁴ the linear and non-linear parameters of the model are fitted. The whole spectrum is fitted simultaneously thus avoiding discontinuities in the fit of the continuum.

The version HEX78 contains five non-linear parameters, four of which describe the calibration and resolution of the peaks (see Table 1). The fifth non-linear parameter P_5 is the area of the analysed sample and is fitted when analysing spot samples of unknown area, to facilitate a correct self-absorption correction. The background function retains 10 linear parameters (see Table 1) and 35 other linear parameters are reserved for the elements fitted. The increase in background for all energies lower than the peak energy due to low energy tailing is partly taken care of by including a step function in the model. The low energy tail close to the peak is, however, not included in the model.

Table 1. List of the functions in the HEX78 version of the program for energy calibration, detector resolution and the continuum^a

Energy calibration	$E = P_1 + P_2 \cdot Z$
Resolution of the detector	$\text{FWHM} = \sqrt{P_3^2 + P_4^2} \cdot E$
Continuum	$\text{CONT} = \text{CONT1} + \text{CONT2}$
	$\text{CONT1} = T \cdot \text{EXP}(-P_2 C_1 Z) (P_6 Z + P_7 Z^2 + P_8 Z^3 + P_9 Z^4)$
	$\text{CONT2} = P_{10}/E + P_{11} + T \cdot (P_{12} + P_{13} Z + P_{14} Z^2 + P_{15} Z^3)$

^a Z = Channel number I minus a fixed reference channel; E = x-ray energy; FWHM = full width at half maximum; T = transmission through the system; C_1 = a constant; P_i = parameters.

Before starting the fitting, an element library is read from a data file. This library contains information including the mass absorption coefficients and x-ray peaks of each element. For a particular x-ray peak, its energy and relative intensity compared to other peaks of the same element are included. Information about the elements to be requested in the spectrum, starting values of the non-linear parameters and the experimental conditions (e.g. absorber and beam area) are also given.

HEX78 Fits first the linear parameters using the fixed starting values of the non-linear parameters (P_1 – P_5). This is followed by a number of fits of both linear

CCC-0049-8246/82/0011-0194\$03.50

and non-linear parameters. This fitting procedure is interrupted when one of the following conditions is satisfied: the reduced χ^2 , the absolute value of each component of the vector $\nabla\chi^2$ or the relative change of all the parameters is less than preset values or if a maximum number of iterations has been performed. Finally, another fit of the linear parameters is made.

ESCAPE PEAKS

When an incident x-ray photon of energy E creates a vacancy in the K shell of a silicon atom in a Si(Li) detector, the emission of either a photoelectron or a Si K x-ray photon (energy = E_{Si}) may result. If the Si x-ray photon escapes from the sensitive volume of the crystal, the resulting voltage pulse from the detector system is proportional to $(E - E_{\text{Si}})$ rather than E . This phenomenon creates a peak in the x-ray spectrum with an energy $E - 1.739$ keV (E Si K α = 1.739 keV) and with the same full width at half maximum (FWHM) as an ordinary x-ray peak at energy $E - E_{\text{Si}}$. Since the escape peak and parent peak are created by the same initial x-ray photon, the ratio between the area of the escape peak and its parent peak is independent of absorption effects. The intensity of Si K β is only 0.0294⁵ of that of Si K α and the energy of Si K β is 1.836 keV and thus the escape peak from Si K β is included in the Si K α escape peak. If the detector is well-collimated and the detector crystal sufficiently deep, losses only occur through the front surface of the crystal.

Theoretical calculations

Assuming an infinitely deep and infinitely wide detector and x-rays incident perpendicular to the surface of the detector, the following formula can be derived for the fraction ε of the emitted Si K radiation which escapes from the detector:^{6,7}

$$\varepsilon = \frac{1}{2} \cdot [1 - \mu_{\text{Si}}/\mu_i \cdot \ln(1 + \mu_i/\mu_{\text{Si}})] \quad (1)$$

Here μ_i is the photoelectric mass absorption coefficient in Si for the incident radiation and μ_{Si} the photoelectric mass absorption coefficient in Si for Si K radiation.

The escape ratio η (the number of counts in the escape peak per total number of counts in the escape peak and the full energy peak) is then equal to

$$\eta = \omega_k \cdot (r - 1)/r \cdot \varepsilon$$

where ω_k is the K shell fluorescence yield of Si and r the K absorption edge jump ratio.

The intensity (κ) of the escape peak to the parent peak is $\kappa = \eta/(1 - \eta)$.

If the x-rays are not incident perpendicular to the surface of the detector, formula (1) is changed to⁸

$$\varepsilon = \frac{1}{2} \cdot \{1 - \mu_{\text{Si}} \cdot \cos \theta / \mu_i \cdot \ln[1 + \mu_i / (\mu_{\text{Si}} \cdot \cos \theta)]\} \quad (2)$$

where θ is the angle between the incident x-rays and the normal to the front surface of the detector.

In calculating theoretical values of the escape ratios,

Table 2. A comparison between the values of the escape ratios from theoretical calculations and from the curve ($\eta = 0.0614/E - 0.00858 + 0.000347 \cdot E$) fitted to the experimental data, the error bars indicate one SD

Energy (keV)	Escape ratio (η)		$\eta_{\text{theor}}/\eta_{\text{exp}}$
	Theory	Experiment	
4	$0.00791 \pm 10 \%$	$0.00816 \pm 2 \%$	0.969
5	$0.00527 \pm 11 \%$	$0.00544 \pm 1 \%$	0.969
6	$0.00355 \pm 12 \%$	$0.00374 \pm 1 \%$	0.949
8	$0.00174 \pm 12 \%$	$0.00187 \pm 2 \%$	0.930
10	$0.00094 \pm 13 \%$	$0.00104 \pm 5 \%$	0.904

mass absorption coefficients from Veigele⁹ are used. The value of ω_k used is 0.0482¹⁰ and of $(r - 1)/r$, 0.918.⁹ Table 2 shows the calculated values of the escape ratios assuming perpendicular incidence of the x-rays. The theoretical calculations are affected by the uncertainty of the fluorescence yield value ($\omega_k = 0.0482 \pm 0.0041$) and the uncertainties of the photoelectric cross sections (2–5 %). At higher x-ray energies, neglect of multiple scattering in the physical model can lead to further errors.

Measurements of escape ratios

The detector used in this work was a 5 mm thick 80 mm² Kevex Si(Li)-detector with a FWHM of 158 eV at 5.9 keV. To avoid incomplete charge collection at the edge of the detector crystal, a Ta-aperture was placed in front of the detector thus reducing its effective sensitive area from 80 mm² to about 30 mm².¹¹ The geometry of the detector and the sample is shown in Fig. 1. Since the transmission through a 5 mm thick Si-crystal is less than 10^{-4} for x-rays with energies below 15 keV, escape from the rear of the crystal can be neglected. Compared to the mean free path of Si x-rays, the dimensions of the crystal can be considered as infinite.

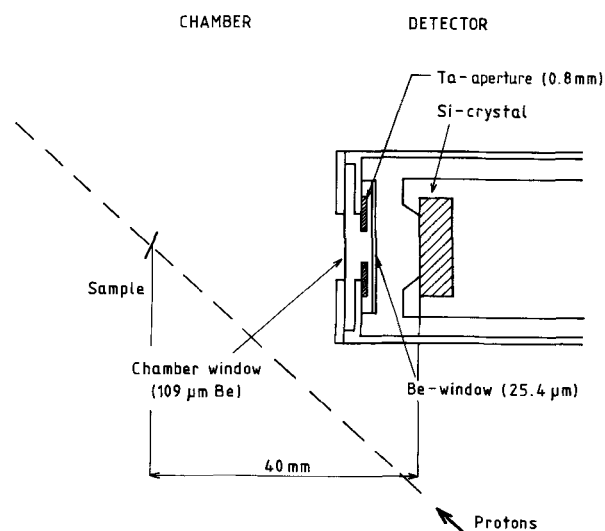


Figure 1. The geometry of the detector arrangement in the Lund PIXE set-up.

For the geometry shown in Fig. 1 and with an 8 mm proton beam collimator, the angles θ of all x-rays reaching the detector is less than 8° . Calculations of ϵ using formulae (1) and (2), respectively, for this angle will give less than a 1 % difference between the results. Hence, for the geometry in question, the dependence on angle θ can be neglected.

Thin homogeneous single element standard foils were irradiated to get good counting statistics in the escape peaks (normally >5000 counts). The library of the HEX program was extended to include extra peaks for the escape peaks of interest. The escape peaks and the parent peaks were fitted independently using the HEX program. In Fig. 2 the measured escape ratios η versus the x-ray energy of the full energy peaks are plotted. By using least squares fits, two different curves have been fitted to the measured values. The first fit based on the physical model of the escape ratio is⁸

$$\eta = C_1(1 - C_2 E^{C_3} \ln(1 + 1/(C_2 E^{C_3}))) \quad E > 1.84 \text{ keV} \quad (3)$$

The values of C_1 , C_2 and C_3 found by the non-linear least squares fit were 0.0226, 0.0141 and 2.86. This value of C_1 (0.0226) should be compared to that used for the theoretical calculations ($C_1 = 1/2 \cdot \omega_k \cdot (r-1)/r = 0.0221$). The value of reduced χ^2 obtained from the fit was 0.695.

A simplified model

$$\eta = C_1/E + C_2 + C_3 \cdot E \quad 3.3 \text{ keV} < E < 10.6 \text{ keV} \quad (4)$$

was also fitted to our measured values (reduced $\chi^2 = 0.811$). This model can be compared to the model $\kappa = \eta/(1 - \eta) = C_1/E + C_2 + C_3 \cdot E + C_4 \cdot E^2$ suggested by Reed and Ware.¹² The deviation of the results between the two fitted curves is shown in Fig. 3. Agreement in the energy interval of interest (3.3–10.6 keV) is very good with a maximum deviation of

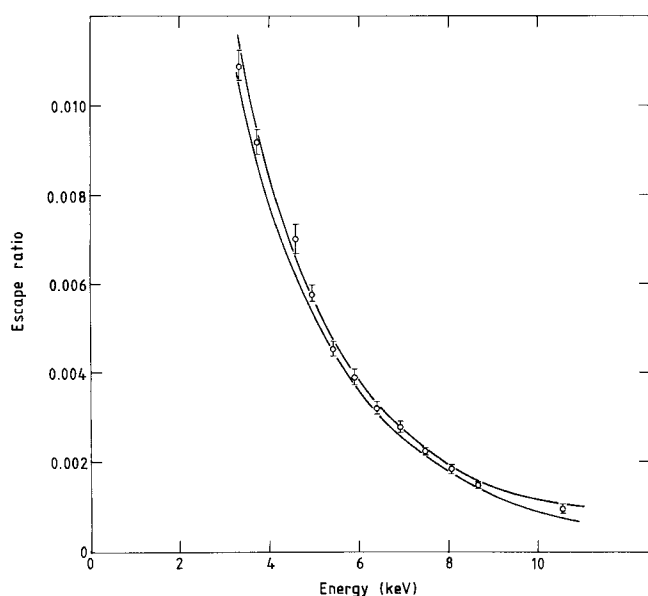


Figure 2. The measured escape ratios (\pm one SD) as a function of the energy of the incident x-rays. In the diagram the 95 % confidence interval around the fitted function $\eta = 0.0614/E - 0.00858 + 0.000347 \cdot E$ is also shown.

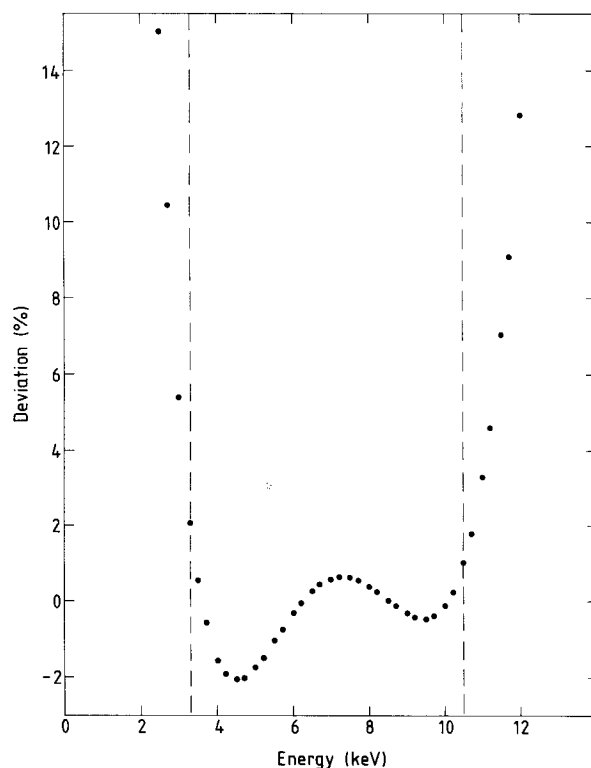


Figure 3. The relative difference between the escape ratios obtained from the two fitted curves $\eta = 0.0614/E - 0.00858 + 0.000347 \cdot E$ and $\eta = 0.0226(1 - 0.0141 \cdot E^{2.86} \cdot \ln(1 + 1/(0.0141 \cdot E^{2.86})))$ as a function of energy E .

2 %. Since the statistical analysis is simplified and the deviation of the results in the two models so small, the fit of model (4) will be used in the following discussions. It is, however, impossible to use the simplified model outside this energy interval (see Fig. 3). The 95 % confidence interval for the fitted values of the escape ratios η has been calculated and is also shown in Fig. 2.

In Table 2 the results from the fitted curve are compared to the theoretical values calculated.

The results of the determination of the relative intensities of the escape peaks to their parent peak (κ) are compared in Table 3 with results from Refs 7 and 13. Reed and Ware⁷ used a detector with an active area of 12.6 mm^2 and a depth of 3.64 mm and Sioshansi and Lodhi¹³ a 5 mm thick collimated 80 mm^2 detector (a set of two collimators 7 mm and 3 mm at a distance of 5.0 cm and 3.5 cm from the detector crystal was used). The agreement between the results of this work and those obtained by Sioshansi and Lodhi is excellent, except for potassium. For most elements the values from Reed and Ware are 10 % or more lower. However, considering the uncertainties, the agreement is fairly good.

Escape peaks in the computer program

If the escape peaks in an x-ray spectrum are not fitted, erroneous results will occur because of the interferences between escape peaks from major x-ray lines and full energy peaks from minor components. An

Table 3. The size of the escape peak area to the full energy peak area for different elements, for comparison, the results from Refs 7 and 13 are given

Detected K α -line	The relative size of the escape peak		
	This work (fitted value)	Reed and Ware ⁷	Sioshansi and Lodhi ¹³
K	0.0111 \pm 0.00021		0.00985 \pm 0.00020 (K α + K β)
Ca	0.00934 \pm 0.00016	0.0071 \pm 0.0003	0.00805 \pm 0.00040
Sc	0.00786 \pm 0.00012		0.00774 \pm 0.00008
Ti	0.00660 \pm 0.00009	0.0058 \pm 0.0002	0.00661 \pm 0.00020
V	0.00554 \pm 0.00007	0.0053 \pm 0.0002	0.00526 \pm 0.00010
Cr	0.00465 \pm 0.00006	0.0043 \pm 0.0003	0.00468 \pm 0.00007
Mn	0.00388 \pm 0.00005	0.0033 \pm 0.0005	0.00384 \pm 0.00008
Fe	0.00324 \pm 0.00005	0.0030 \pm 0.0001	0.00293 \pm 0.00006
Co	0.00269 \pm 0.00004	0.0021 \pm 0.0003	0.00273 \pm 0.00008
Ni	0.00223 \pm 0.00004	0.0017 \pm 0.0003	0.00229 \pm 0.00011
Cu	0.00185 \pm 0.00004		0.00175 \pm 0.00005
Zn	0.00153 \pm 0.00004	0.0013 \pm 0.0004	0.00158 \pm 0.00006
As	0.00091 \pm 0.00007		0.00108 \pm 0.00006

example is the iron content in a welding fume sample which gives rise to an escape peak at 4.66 keV, thus interfering with Ti which is often found in rather low concentrations in welding fumes. Another example is the problem of obtaining reliable results for phosphorous in biological material because of interference with the escape peaks of Ca K α and K K β . Using values of the escape ratios found by fitting the parameters of the simple model (4) described above, the size of the escape peaks relative to the parent peaks (κ) have been calculated for all x-ray peaks in the energy interval 3.3–10.6 keV. The ratios of the escape peaks at lower energies are of less interest since x-ray peaks are not detected in that energy region. The size of the escape peaks from x-ray lines above 10.6 keV is usually small due to decreasing cross sections for the production of x-rays in the sample and decreasing escape ratios with increasing x-ray energy.

The relative intensities of the escape peaks to their parent peak (κ) are added to the information on the peaks in the HEX library. Since the computer program works from higher to lower x-ray energies in constructing the physical model, the following technique suggested by Reed and Ware¹² is used. An image of the x-ray peak, modelled and multiplied by the relative size of the escape peak is added to the model at an energy 1.74 keV below the parent x-ray peak. This is a very fast and convenient way of including the escape peaks in the computer fit. It gives peaks with correct transmission and area but of a somewhat erroneous width. The difference in FWHM is, however, so small (e.g. for Fe K α the difference is about 20 eV) that for practical analytical work it can be neglected.

PILE-UP PEAKS

When two photons reach the x-ray detector within a certain time interval, the corresponding pulses may be fully or partially added in the amplifier. In the case of complete addition, pile-up peaks appear at an energy which is equal to the sum of the individual energies.

The pile-up effect can be reduced by using an electronic pile-up rejector system, a beam deflection system or a combination of both systems. The system used in the Lund PIXE-facility for obtaining a pile-up interval of about 250 ns is described by Malmqvist *et al.*¹⁴

The count rate N of the pile-up peak emanating from adding pulses corresponding to x-rays of energy A and B is

$$N = 2\tau N_A N_B$$

The count rate of the pile-up peak when A is equal to B is

$$N = \tau N_A^2$$

where τ is the pile-up interval and N_A , N_B the number of pulses corresponding to x-rays of energy A and B per unit live time, respectively.

To be able to calculate the size of a pile-up peak by using the formulae above or a more general formula suggested by Steinbauer,¹⁵ the current has to be constant during the irradiation. The formulae also require a known pile-up interval τ .

To incorporate the pile-up peaks in the HEX fitting routine, another approach to the solving of the problem has been chosen which is not dependent on a constant count rate during the irradiation of the sample or a known value of τ . In Fig. 4 a flow chart of the technique used is shown. The first linear fit to the spectrum is performed without the pile-up peaks. The peaks are sorted and the i largest peaks selected for the continued calculations. The number i can be changed depending on the application. If the energies of two peaks differ less than 50 eV, they are considered as one peak. The relative intensities and energies are calculated for all the possible pile-up peaks (number of pile-up peaks = $i(i+1)/2$). The m largest pile-up peaks are then selected. The number m can also be varied. Knowing the relative intensities and energies of these m pile-up peaks, they can be added to the library of HEX as one special 'pile-up element' including all the pile-up peaks chosen. By treating the pile-up peaks as a special element with fixed relative intensities between the peaks, the interferences with

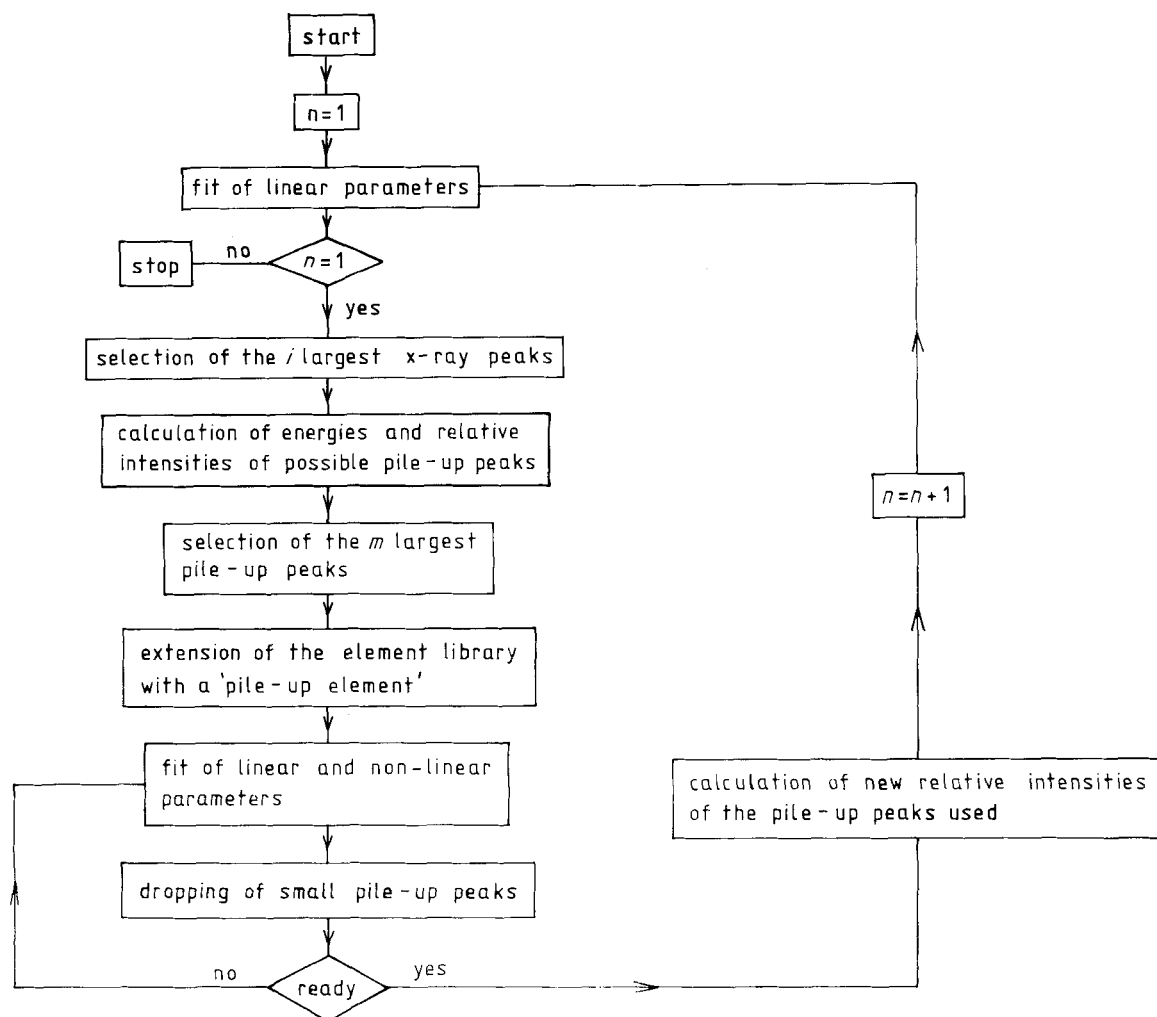


Figure 4. A flow chart of the routine used for fitting pile-up peaks.

other x-ray peaks can be resolved. The relative intensity of each pile-up peak is adjusted by a factor to give correct results since in the fitting routine they will be regarded as normal x-ray peaks with transmissions different from those which the pile-up peaks have. In the following iterations, the 'pile-up element' is treated exactly in the same way as other elements which have been requested, e.g. too small pile-up peaks are dropped. When one of the various conditions for finishing the fitting procedure is fulfilled (see above) and prior to performing the last linear fit, the relative intensities of the escape peaks are recalculated from the actual areas of the x-ray peaks and these updated values are used in the last linear fit.

Experience of the fitting of pile-up peaks

The technique developed works very satisfactorily and has significantly improved the HEX-analysis. An example of a spectrum fitted with and without the pile-up peak routine is shown in Fig. 5. The sample (welding fumes from stainless steel welding collected on a Millipore filter) was irradiated for about 20 min. The count rate was about 5000 counts/s and a beam deflec-

tion system having a 400 ns pile-up interval was used. The spectrum can be considered as being extremely complicated in having many almost equally large x-ray peaks. For the fit, the 40 largest pile-up peaks originating from the 12 largest x-ray peaks of the spectrum were used. The fitting of the spectrum can, in this particular case, be improved further by including even more pile-up peaks. The difference between data and fitted values around channel 440 is an example of missing pile-up peaks ($\text{Fe}\alpha + \text{Ni}\beta$ and $\text{Fe}\beta + \text{Ni}\alpha$). In Table 4 are presented results from the two computer analyses. It should be observed that only elements frequently appearing in welding fume samples were asked for in the request list. Analysing a completely unknown sample, even more false elements would have been fitted if the pile-up peaks had not been included in the computer code. In many applications a lower number of pile-up peaks is sufficient to obtain a good fit.

The expected value of the energy of a pile-up peak is the sum of the energies of its two parent peaks. The pile-up peaks in Fig. 5 are, however, observed at somewhat higher energy (+30 eV). The apparent increase in energy for pile-up peaks in our set-up may be explained by a negative plateau observed on the pulses at the output of the main amplifier.

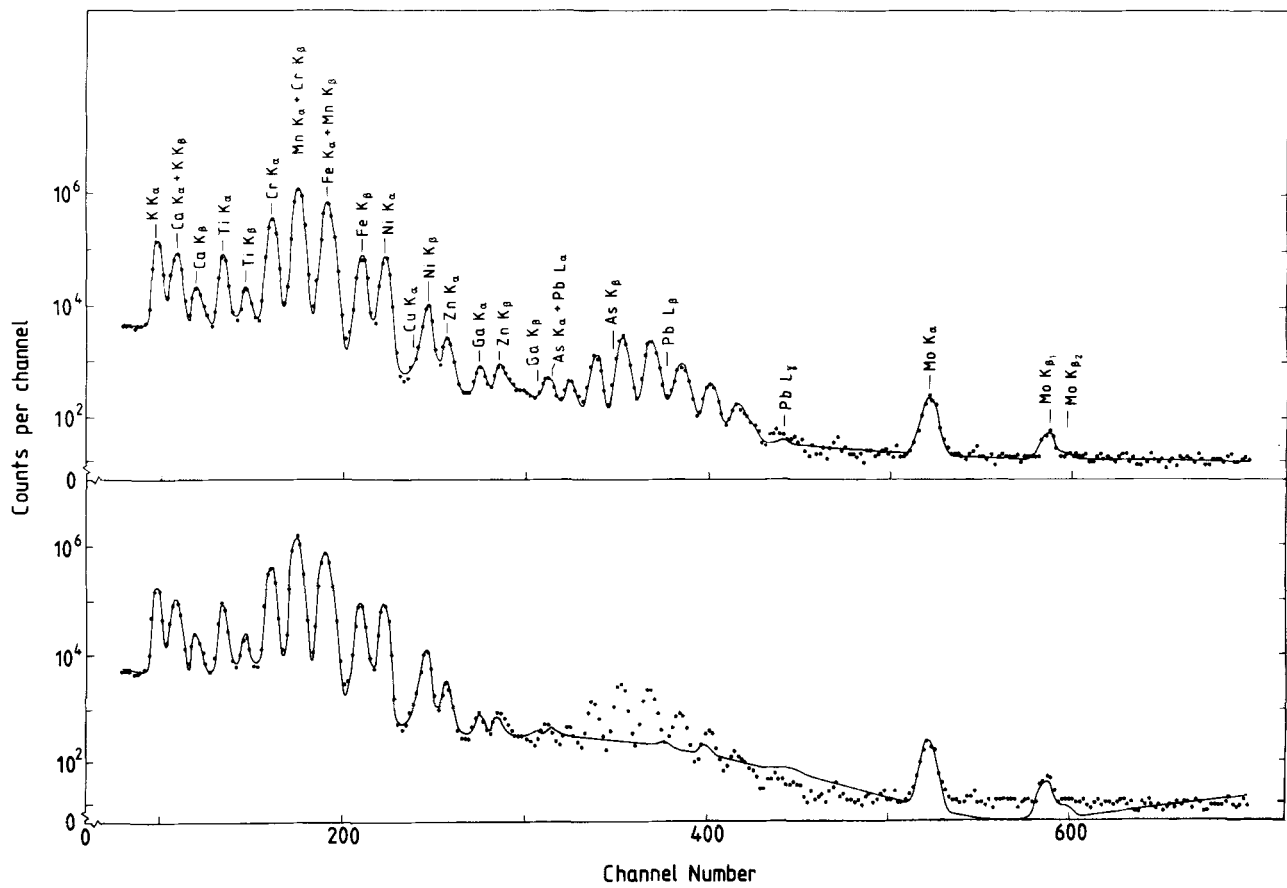


Figure 5. A PIXE-spectrum from the analysis of a welding fume sample fitted with (top) and without (bottom) the inclusion of the pile-up routine in the computer program. The elements detected are indicated in the spectrum (top). The sample was irradiated for about 20 min using a count rate of 5000 counts/s.

The combination of good electronics to suppress pile-up peaks and an effective computer program to handle the remaining peaks facilitates the use of an increased count rate.

Table 4. The results of elemental mass calculations from the computer analysis of a welding fume sample (see Fig. 5) when the spectrum is fitted with and without the pile-up routine

Element	Amount ($\mu\text{g cm}^{-2}$) (pile-up routine not included)	Amount ($\mu\text{g cm}^{-2}$) (pile-up routine included)
K	55.9	56.0
Ca	15.7	15.4
Ti	7.24	7.26
Cr	24.9	25.0
Mn	82.3	82.4
Fe	37.8	37.7
Ni	7.40	7.37
Cu	0.0738	0.0649
Zn	0.422	0.416
Ga	0.0897	0.0387
As	<0.021	0.0397
Rb	0.0904	<0.048
Mo	0.997	0.893
Pb	0.129	0.122

PEAK DROPPING

To obtain a good fit of an x-ray spectrum, all possible elements for the kind of sample analysed have to be included in the request list of the computer program. This will, however, normally cause the program to fit a lot of extremely small peaks which is very time consuming. A routine for dropping small peaks is, therefore, included in the computer code. In earlier versions of HEX, all peaks containing less than four counts were deleted from the list of the energies of the peaks. The peaks dropped are not fitted in the next iteration and computer time significantly reduced. This way of dropping peaks can, however, give rise to erroneous results, e.g. if all but one peak of an element has been dropped and this remaining peak interferes with another element. Such problems have been observed for Mo and S, when all Mo peaks except one L peak are dropped. The Mo peak may then get too large value at the expense of the S peak.

To avoid this kind of problem, the rejection sub-routine has been improved. Two suitable peaks (e.g. $K\alpha$ and $K\beta$) from each element are marked not to be dropped unless the entire element is dropped. This way of dropping peaks works satisfactorily in reducing the number of peaks and still largely avoids the problems described above.

PLANNED IMPROVEMENTS

The HEX program was originally developed for thin target analysis, but it is now also used routinely for determining the peak areas of different elements in thick samples. For all matrices of interest, special libraries with adjusted relative intensities of the peaks are calculated. A special computer program TJOCKT¹⁶ is then used for evaluating the elemental composition of the sample. To make routines to handle thick samples easier and faster, the inclusion of this thick target procedure in the HEX program is planned.

A problem still not completely solved in the HEX program is that of the low energy tails on the x-ray peaks. As discussed above, the detector crystal is collimated to a sensitive area of about 30 mm². This collimation reduces the tails significantly¹¹ but small nonexistent peaks may still be fitted close to a large x-ray peak to compensate for the remaining tail. We plan to make changes in the program so as to include the tails in the physical model. Different ways of handling the tails have been suggested in the literature.¹⁷⁻²⁰

CONCLUSION

The HEX program has been improved by including escape peaks and pile-up peaks in the computer code

and developing an effective routine for dropping very small x-ray peaks.

The measured escape ratios are in good agreement with theoretical calculations and the findings of other experimental groups. The computer code works by subtracting the escape peak from the x-ray spectrum as an image of the parent peak, giving very accurate analytical results.

The relative intensities and energies of the largest pile-up peaks are calculated and fitted to the spectrum as a special 'pile-up element'. This approach works independently of count rate and the setting of the electronics for pile-up suppression. Since the relative intensities of the pile-up peaks are fixed, interferences with other peaks can be resolved. The inclusion of pile-up peaks in the computer code facilitates the use of an enhanced rate and thus a higher analysis speed.

Acknowledgement

I am indebted to Mr H. C. Kaufmann, Tallahassee, USA, for his many creative ideas and his active participation in the initial phase of this project. Dr K. R. Akselsson has been a never-ceasing source of ideas and stimulation throughout the whole work, for which I am indeed grateful. I am also very grateful to Dr K. Malmqvist for many helpful discussions about this work.

REFERENCES

1. H. C. Kaufmann and K. R. Akselsson, *Adv. X-Ray Anal.* **18**, 353 (1975).
2. H. C. Kaufmann, K. R. Akselsson and W. J. Courtney, *Adv. X-Ray Anal.* **19**, 355 (1976).
3. H. C. Kaufmann, K. R. Akselsson and W. J. Courtney, *Nucl. Instrum. Methods* **142**, 251 (1977).
4. D. W. Marquardt, *J. Soc. Indust. Appl. Math.* **11**, 431 (1963).
5. J. H. Scofield, *Phys. Rev. A* **9**, 1041 (1974).
6. P. Axel, *Rev. Sci. Instrum.* **25**, 391 (1945).
7. S. J. B. Reed and N. G. Ware, *J. Phys. E* **5**, 582 (1972).
8. P. J. Statham, *J. Phys. E* **9**, 1023 (1976).
9. W. M. J. Veigele, *Atomic Data Tables* **5**, 51 (1973).
10. A. Langenberg and J. van Eck, *J. Phys. B* **12**, 1331 (1979).
11. K. G. Malmqvist, G. I. Johansson and K. R. Akselsson, to be published in *J. Radioanal. Chem.*
12. S. J. B. Reed and N. G. Ware, *X-Ray Spectrom.* **2**, 69 (1973).
13. P. Sioshansi and A. S. Lodhi, *X-Ray Spectrom.* **8**, 65 (1979).
14. K. G. Malmqvist, E. Karlsson and K. R. Akselsson, *Nucl. Instrum. Methods* **192**, 523 (1982).
15. E. Steinbauer, *Nucl. Instrum. Methods* **181**, 21 (1981).
16. L.-E. Carlsson, J. Pallon and K. R. Akselsson, private communications.
17. P. van Espen, H. Nullens and F. Adams, *Nucl. Instrum. Methods* **145**, 579 (1977).
18. L. A. McNelles and J. L. Campbell, *Nucl. Instrum. Methods* **127**, 73 (1975).
19. H. H. Jorch and J. L. Campbell, *Nucl. Instrum. Methods* **143**, 551 (1977).
20. E. Clayton, D. D. Cohen and P. Duerden, *Nucl. Instrum. Methods* **180**, 541 (1981).

Received 5 August 1981; accepted 2 June 1982